

Analysis of IUE spectra of helium-rich white dwarf stars[★]

B. G. Castanheira¹, S. O. Kepler¹, G. Handler^{2,3}, and D. Koester⁴

¹ Instituto de Física, Universidade Federal do Rio Grande do Sul, 91501-900 Porto-Alegre, RS, Brazil
e-mail: barbara@if.ufrgs.br

² Institut für Astronomie, Universität Wien, Türkenschanzstrasse 17, 1180, Wien, Austria

³ South African Astronomical Observatory, PO Box 9, Observatory 7935, South Africa

⁴ Institut für Theoretische Physik und Astrophysik, Universität Kiel, 24098 Kiel, Germany

Received 17 September 2005 / Accepted 30 December 2005

ABSTRACT

We studied the class of DB white dwarf stars, using re-calibrated UV spectra for thirty four DBs obtained with the IUE satellite. By comparing the observed energy distributions with model atmospheres, we simultaneously determine spectroscopic distances (d), effective temperature (T_{eff}), and surface gravities ($\log g$). Using parallax measurements and previous determinations of T_{eff} and $\log g$ from optical spectra, we can study whether the atmospheres of eleven DB stars are consistent with pure He or have a small amount of H contamination. We also report on our observations of seventeen stars with T_{eff} close to the DB instability strip through time series photometry and found them to be non variable within our detection limits.

Key words. stars: white dwarfs – stars: variables: general – stars: oscillations – ultraviolet: stars

1. Introduction

Among all known white dwarf stars, around 20% have a helium (He) dominated atmosphere, and are thus assigned the spectral type DB. Most of these stars are believed to be result of the born again or a very late He thermal pulse during the early planetary nebula cooling phase (e.g. Althaus et al. 2005). In this event, the residual hydrogen (H) is completely burnt, the star returns quickly to AGB phase and again to planetary nebula, this time, without H. As they stars cool down, DBs cross an instability strip, where they are seen as multi-periodic pulsators. Beauchamp et al. (1999) determined its boundaries as $27\,800 \geq T_{\text{eff}} \geq 22\,400$ K from a comparison of their pure He model atmosphere grid with $ML2/\alpha = 1.25$ to optical spectra, and $24\,700 \geq T_{\text{eff}} \geq 21\,800$ K, if undetectable traces of hydrogen (H) are allowed in the models.

The study of the instability strip of the DBs is still a challenge because of the small number of known pulsators; only seventeen are known to date (Nitta et al. 2005). Another difficulty is that the determinations of T_{eff} and $\log g$ from spectra are degenerate as, in general, these two parameters are correlated. Working with optical spectra is even more problematic, as possible contamination with even trace amounts of hydrogen that are undetected in the spectra can decrease the resulting effective temperatures by up to 3000 K and $\log g$ by up to 0.05 dex (Beauchamp et al. 1999). The uncertainty in T_{eff}

derived from the published optical spectra is thus comparable to the width of the instability strip.

The DBs have been studied since the 1960 s, but especially after the discovery of a pulsator, GD 358, based on theoretical predictions (Winget et al. 1982). This star is the brightest and one of the best studied variable He atmosphere white dwarf (DBV) stars. Because pulsation theory gives detailed predictions of DBV properties, these stars can be used to study neutrino rates probing the electro-weak theory (Winget et al. 2004; Córscico & Althaus 2004), the $C(\alpha, \gamma)\text{O}$ cross section (Metcalf 2003, 2005), and the He^3/He^4 separation (Wolff et al. 2002; Montgomery & Winget 2000) which cannot be achieved in any terrestrial laboratory. Pulsations in DBs are predicted to exist in a narrow temperature range, ~ 3000 K wide, but it has been difficult to measure T_{eff} with sufficient accuracy to determine the edges of the instability strip.

Considerable interest is focused on the accurate determination of atmospheric parameters for DB white dwarfs, for yet another reason, the so called “DB gap”, where there are no observed DB stars. It occurs between 45 000 and 30 000 K in the cooling sequence (e.g. Hansen & Liebert 2003). The physical reason of the DB gap is still not understood. However, many theories attempt to explain why there would be no DBs within this range of temperature. One possibility is that DBs would turn into DAs (white dwarf with pure H atmospheres) by dragging H to the surface of the star, blocking the atmosphere. In this scenario, we expect to find more H in the hot DBs than

[★] Partially based on observations at Observatório do Pico dos Dias/LNA.

in the cooler ones. We also investigate that possibility in this paper, but we do not confirm this theory.

2. Fitting the ultraviolet spectra

To study the DBs as a class and the characteristics of their instability strip, we used ultraviolet spectra because they are less affected by possible trace amounts of H that plague the optical determination of the effective temperature (Beauchamp et al. 1999). The data we use to determine the distance (d), effective temperature (T_{eff}), and surface gravity ($\log g$) are the re-calibrated ultraviolet spectra for DB stars, obtained with the International Ultraviolet Explorer (IUE) satellite and published by Holberg et al. (2003). The spectra were re-calibrated with the New Spectroscopic Image Processing System (NEWSIPS) data reduction by NASA, and in the low-dispersion spectral mode with a resolution of $\sim 6 \text{ \AA}$.

One of the major motivations to use the archive of IUE low-dispersion spectra, besides it comprising an homogeneous sample, is to work with spectra of which the absolute calibration is based on a synthetic model atmosphere energy distribution for the white dwarf star G191-B2B (WD 0501+527). The models we fit are the same kind used in the flux calibration.

We used a new grid of Koester's model atmospheres, with input physics and methods similar to those described in Finley et al. (1997), consisting of models with T_{eff} from 12 000 K to 28 000 K, and a step of 500 K, and $\log g$ from 7.0 to 9.0, with 0.1 dex step. We used two sets of model atmospheres: pure He and He contaminated with a small amount of H [$\log y \equiv \log(N\text{He}/N\text{H}) = -3.0$]. This is the the upper limit for the amount of H contamination for a star not show discernible H lines in the optical spectra, i.e., to be classified as a DB and not as a DBA. All models were calculated with $ML2/\alpha = 0.6$ mixing length theory, considering that Bergeron et al. (1995) and Koester & Vauclair (1997) have shown this choice of mixing length gives consistent results in the UV and optical, for the DAs. There is no reason to expect the mixing length description to be different for DBs. These models were used to simultaneously fit T_{eff} , $\log g$ and d to the available IUE spectra.

We calculated the minima in χ^2 between the observed spectra and the models, allowing the three parameters, T_{eff} , $\log g$, and d , to vary. We used the model radii described in Althaus & Benvenuto (1997), available in <http://www.fcaglp.unlp.edu.ar/evolgroup/tracks.html>.

Our determinations of T_{eff} , $\log g$ and the distance for all DB stars with IUE spectra available are shown in Table 1. In Cols. 3–5, we show the values derived using pure He models, and in Cols. 6–8, the same parameters using He/H models.

3. Comparison of results

Our determinations are still degenerate with respect to the contamination of H in the He atmosphere. To minimize this effect, we used external measurements, like: optical spectra, parallax measurements, and V magnitudes, if available.

3.1. Distance moduli

To test the reliability of our spectroscopic distances, we used our determinations of T_{eff} and $\log g$, Bergeron's et al. (2001) absolute magnitude, and the published V magnitude to estimate the distance moduli. In Table 2 we show the derived distances from this method and the distances after cross correlating both solutions.

In almost all cases, both spectroscopic and magnitude derived distances agree, even though we used independent model grids.

3.2. Parallax measurements

For six stars of our sample, parallax measurements are available (van Altena et al. 2001). Comparing these distances with the ones derived spectroscopically, the better agreement, in general, is the solution derived using pure He models. There are two stars, GD 358 and GD 408, for which we could not distinguish the atmospheric composition. Feige 4 is an exception, for which both spectroscopic solutions do not agree with the published parallax. However, this is the faintest star in our sample with parallax measurement, with magnitude close to the limit of the catalog. In Table 3, we show the parallax distance and the best stellar composition cross correlating the solutions.

The IUE spectra of Feige 4 (full line) is shown in Fig. 1 in comparison to the models. The best models derived from the spectra are with $T_{\text{eff}} = 19\,000 \text{ K}$, $\log g = 8.50$, $d = 61 \text{ pc}$, and pure He (dashed line) and with $T_{\text{eff}} = 18\,000 \text{ K}$, $\log g = 7.50$, $d = 112 \text{ pc}$, and He/H grid (dotted line). Using the distance derived from parallax, $d = 33 \text{ pc}$, the best models are not only much cooler, $T_{\text{eff}} = 14\,000 \text{ K}$ for pure He models (dotted-dashed line) and $T_{\text{eff}} = 17\,000 \text{ K}$ for He/H models (long dashed line), but they also do not fit the slope of the observed spectra. Another argument to claim the parallax measurement is not correct is that this star has apparent magnitude $V = 15.3$, too faint for such a large parallax, unless the radius is extremely small, i.e., high mass, incompatible with the observed spectra.

3.3. Comparison with optical spectra results

Beauchamp et al. (1999) studied the optical spectra of eight known DBVs together with fifteen other DB and DBA stars with temperatures above 20 000 K. For DBs, including DBVs, they used a pure He atmosphere composition, or a homogeneous H/He ratio with only traces of H, at the detection threshold – defined as that which would produce barely visible H β or H γ features, two lines included in their spectra. The influence of small, spectroscopically invisible amounts of H in the DB's atmospheres is an important issue in the definition of the temperature scale in the optical, because T_{eff} determined using He models with small admixture of H are often lower by a few thousand of K, than those determined with pure He models.

The instability strip Beauchamp et al. (1999) derived from the analysis of optical spectra contains non-variable stars. Its T_{eff} is also uncertain due to the possible presence of trace amounts of H in the stellar atmospheres. In Table 4, we compare our determination for T_{eff} from UV spectra, described

Table 1. Atmospheric parameters and distance determined from IUE spectra, using pure He models (He) and He contaminated with a small amount of H (He/H) models. An asterisk indicates a DBA star, for which our determinations are not adequate.

Name	WD	He T_{eff} (K)	He $\log g$	He d (pc)	He/H T_{eff} (K)	He/H $\log g$	He/H d (pc)
G 266-32	0000-170	16 000 \pm 600	8.50 \pm 0.60	39 \pm 12	14 000 \pm 270	8.00 \pm 0.02	46 \pm 3
GD 408	0002+729	14 000 \pm 40	8.50 \pm 0.04	26 \pm 1	14 000 \pm 40	7.50 \pm 0.07	54 \pm 2
Feige 4	0017+136	19 000 \pm 170	8.00 \pm 0.17	61 \pm 5	18 000 \pm 60	7.50 \pm 0.06	112 \pm 7
G 270-124	0100-068	20 500 \pm 130	8.40 \pm 0.23	34 \pm 4	19 000 \pm 100	7.00 \pm 0.15	69 \pm 5
PG 0112+104	0112+104	27 000 \pm 110	7.50 \pm 0.03	136 \pm 2	27 000 \pm 130	8.50 \pm 0.06	71 \pm 2
GD 40	0300-013	15 000 \pm 420	7.50 \pm 0.21	104 \pm 11	15 000 \pm 310	8.50 \pm 0.16	58 \pm 5
BPM 17088	0308-565	21 500 \pm 190	7.70 \pm 0.08	58 \pm 2	21 000 \pm 280	8.00 \pm 0.14	49 \pm 3
BPM 17731	0418-539	20 000 \pm 140	8.00 \pm 0.14	83 \pm 6	19 000 \pm 110	7.50 \pm 0.06	110 \pm 3
BPM 18164	0615-591	16 000 \pm 50	8.50 \pm 0.17	26 \pm 2	16 000 \pm 40	7.00 \pm 0.04	64 \pm 1
Ton 10	0840+262	21 000 \pm 90	7.50 \pm 0.09	96 \pm 4	18 000 \pm 100	7.00 \pm 0.15	103 \pm 8
L748-70	0845-188	18 000 \pm 140	7.50 \pm 0.14	129 \pm 9	18 000 \pm 60	7.50 \pm 0.06	135 \pm 4
PG 0853+163*	0853+163	21 000 \pm 450	7.70 \pm 0.18	126 \pm 11	20 000 \pm 650	7.50 \pm 0.65	137 \pm 44
PG 0948+013	0948+013	19 000 \pm 280	8.20 \pm 0.19	92 \pm 9	18 000 \pm 150	7.00 \pm 0.15	173 \pm 13
GD 303	1011+570	18 000 \pm 140	7.50 \pm 0.14	75 \pm 5	18 000 \pm 60	7.50 \pm 0.03	78 \pm 1
PG 1115+158	1115+158	23 000 \pm 500	8.50 \pm 0.10	137 \pm 7	22 000 \pm 500	7.00 \pm 0.25	321 \pm 40
PG 1149-133*	1149-133	20 500 \pm 440	7.60 \pm 0.57	161 \pm 46	19 000 \pm 260	7.00 \pm 0.19	196 \pm 19
PG 1311+129*	1311+129	26 500 \pm 450	7.70 \pm 0.05	249 \pm 6	27 000 \pm 280	7.50 \pm 0.14	298 \pm 14
PG 1326-037	1326-037	21 500 \pm 290	8.40 \pm 0.35	81 \pm 14	20 000 \pm 100	8.00 \pm 0.10	100 \pm 5
GD 325	1333+487	16 000 \pm 40	8.20 \pm 0.01	34 \pm 0.2	15 000 \pm 120	7.00 \pm 0.06	61 \pm 2
PG 1351+489	1351+489	22 500 \pm 190	7.60 \pm 0.15	194 \pm 14	22 000 \pm 150	7.00 \pm 0.07	266 \pm 10
PG 1411+218	1411+218	15 000 \pm 70	7.80 \pm 0.01	49 \pm 0.3	14 000 \pm 70	7.00 \pm 0.03	66 \pm 1
G 200-39	1425+540	15 000 \pm 110	7.70 \pm 0.09	74 \pm 3	15 000 \pm 310	8.50 \pm 0.31	47 \pm 7
PG 1445+152	1445+152	21 500 \pm 120	8.40 \pm 0.12	91 \pm 5	21 000 \pm 120	8.50 \pm 0.06	86 \pm 3
PG 1456+103*	1456+103	24 000 \pm 190	8.50 \pm 0.27	110 \pm 15	24 000 \pm 290	9.00 \pm 0.14	76 \pm 5
G 256-18	1459+821	16 000 \pm 50	8.00 \pm 0.03	53 \pm 1	15 000 \pm 310	7.00 \pm 0.05	83 \pm 2
GD 190	1542+182	22 500 \pm 90	8.50 \pm 0.11	48 \pm 3	21 000 \pm 60	7.00 \pm 0.06	106 \pm 3
GD 358	1645+325	24 500 \pm 130	8.50 \pm 0.10	29 \pm 1	24 000 \pm 50	8.50 \pm 0.03	30 \pm 0.4
PG 1654+160	1654+160	25 000 \pm 550	7.50 \pm 0.11	237 \pm 13	26 000 \pm 1100	7.00 \pm 0.55	331 \pm 91
L 7-44	1708-871	23 000 \pm 610	8.30 \pm 0.42	55 \pm 12	21 000 \pm 680	7.00 \pm 0.34	106 \pm 18
GD 378	1822+410	17 000 \pm 60	8.20 \pm 0.04	39 \pm 1	16 000 \pm 80	7.00 \pm 0.08	70 \pm 3
L 1573-31	1940+374	17 000 \pm 50	7.60 \pm 0.05	62 \pm 1	17 000 \pm 40	7.00 \pm 0.07	86 \pm 3
BPM 26944	2034-532	17 000 \pm 390	8.50 \pm 0.39	34 \pm 7	17 000 \pm 80	7.00 \pm 0.12	86 \pm 5
G 26-10	2129+000	13 000 \pm 60	7.50 \pm 0.06	50 \pm 2	13 000 \pm 40	7.50 \pm 0.02	54 \pm 1
LTT 9031	2224-344	19 000 \pm 160	7.50 \pm 0.16	72 \pm 6	18 000 \pm 130	7.00 \pm 0.13	88 \pm 6

in Sect. 2, with those derived from optical spectra. The optical spectra also give two solutions, with or without trace H. For seven DB stars, the best agreement in T_{eff} in both UV and optical range is for atmospheres consistent with a small amount of H instead of none. The exception is the star GD 358, which has a higher probability of having a pure He atmosphere in agreement with Provencal et al. (2000) determination of $\log(N_{\text{He}}/N_{\text{H}}) \leq -5$ for this star. In Fig. 2, we show a comparison between UV (x -axis) and optical (y -axis) spectroscopic determinations of T_{eff} , for a pure He atmosphere and a He/H atmosphere. The closer a given data point is to the dashed line (1:1 correspondence between UV and optical spectra), the better the solution for the atmosphere composition becomes. The dotted lines link the two atmosphere determinations for a given star, showing that He/H atmospheres are more likely for this sample.

GD 358 is the only star in our sample which both parallax measurement and optical spectra determination is available. We cannot distinguish the best atmosphere composition from the parallax, but a pure He atmosphere is still consistent with the optical spectra determination.

For the star GD 190, even though we get a better agreement with the optical spectra for a contaminated atmosphere, Provencal et al. (2000) obtained an upper limit of $\log(N_{\text{He}}/N_{\text{H}}) \leq -6.5$, consistent with a pure He atmosphere.

An important consideration is that we fitted all stars using DB models, never with DBA models. From the IUE spectra, we cannot determine if a star is a DBA or not. The optical spectra of PG 0853+163, PG 1149-133, PG 1311+129, and PG 1456+103 do show H, which has been taken into account by Beauchamp et al. (1999) by using models with a considerable amount of H. Our temperatures for DBA stars are

Table 2. Distance determined from distance modulus (Cols. 2–3) using IUE T_{eff} and $\log g$, compared to absolute magnitude models and available V magnitudes. We used both pure He models (He) and He contaminated with a small amount of H (He/H) models. The last 2 columns are the distances after cross correlating these values and the spectroscopic distances (see values in Table 1).

Name	He d (pc)	He/H d (pc)	He d_{cross} (pc)	He/H d_{cross} (pc)
G 266-32	36^{+22}_{-16}	45 ± 2	37^{+13}_{-10}	46 ± 2
GD 408	26 ± 1	51 ± 2	26 ± 1	53 ± 1
Feige 4	81 ± 7	108^{+4}_{-3}	71 ± 4	110 ± 4
G 270-124	35^{+7}_{-6}	88^{+10}_{-9}	34 ± 4	78^{+6}_{-5}
PG 0112+104	144^{+28}_{-20}	71^{+3}_{-4}	140^{+14}_{-10}	71 ± 2
GD 40	100^{+20}_{-15}	50^{+3}_{-8}	102^{+11}_{-9}	54^{+3}_{-5}
BPM 17088	61^{+4}_{-3}	50 ± 5	60 ± 2	50 ± 3
BPM 17731	82 ± 6	109^{+4}_{-3}	83 ± 4	109 ± 2
BPM 18164	27 ± 4	79^{+10}_{-9}	27 ± 2	71^{+5}_{-4}
Ton 10	81^{+4}_{-2}	104^{+9}_{-8}	89^{+3}_{-2}	104 ± 6
L748-70	122^{+14}_{-12}	122^{+6}_{-5}	125^{+8}_{-7}	128^{+4}_{-3}
PG 0853+163*	135^{+18}_{-16}	150^{+95}_{-56}	131^{+11}_{-10}	144^{+52}_{-36}
PG 0948+013	92^{+15}_{-13}	205^{+25}_{-23}	92^{+9}_{-8}	189^{+14}_{-13}
GD 303	119^{+14}_{-11}	119^{+7}_{-3}	97^{+7}_{-6}	98^{+3}_{-1}
PG 1115+158	95^{+8}_{-9}	260^{+53}_{-45}	116^{+5}_{-6}	291^{+35}_{-30}
PG 1149-133*	178^{+92}_{-57}	258^{+42}_{-36}	169^{+51}_{-37}	227^{+23}_{-21}
PG 1311+129*	187 ± 9	218^{+29}_{-22}	218 ± 5	258^{+16}_{-13}
PG 1326-037	82^{+23}_{-22}	103^{+7}_{-8}	82 ± 13	101^{+4}_{-5}
GD 325	$33^{+0.2}_{-0.3}$	70 ± 3	$33^{+0.1}_{-0.2}$	66 ± 2
PG 1351+489	194^{+21}_{-36}	293^{+17}_{-15}	194^{+13}_{-19}	280^{+10}_{-9}
PG 1411+218	$48^{+0.5}_{-0.6}$	76 ± 2	48 ± 0.3	71 ± 1
G 200-39	69^{+5}_{-4}	39^{+11}_{-10}	72 ± 3	43^{+7}_{-6}
PG 1445+152	77 ± 7	71 ± 4	84 ± 4	78 ± 2
PG 1456+103*	87 ± 18	57^{+8}_{-7}	98 ± 12	66 ± 4
G 256-18	60^{+1}_{-2}	111 ± 7	56 ± 1	97 ± 4
GD 190	49^{+4}_{-5}	134 ± 6	49 ± 3	120 ± 3
GD 358	30 ± 2	30 ± 1	30 ± 1	$30^{+0.3}_{-0.4}$
PG 1654+160	196^{+22}_{-16}	302^{+192}_{-113}	216^{+13}_{-10}	317^{+106}_{-73}
L 7-44	57^{+14}_{-12}	133^{+28}_{-22}	56^{+9}_{-8}	119^{+17}_{-14}
GD 378	42 ± 1	90 ± 6	40 ± 1	80 ± 3
L 1573-31	67 ± 2	103 ± 4	64 ± 1	95 ± 3
BPM 26944	34^{+13}_{-11}	101^{+10}_{-9}	34^{+7}_{-6}	93^{+6}_{-5}
G 26-10	58^{+3}_{-2}	58 ± 1	54 ± 2	56 ± 1
LTT 9031	78^{+10}_{-8}	108^{+12}_{-11}	75^{+6}_{-5}	98 ± 6

therefore not reliable, but differences in T_{eff} from our models with or without trace H are the same order as our uncertainties.

We did not compare $\log g$ values, as their uncertainties are too large from both UV and optical spectra.

4. Looking for new pulsators

Robinson & Winget (1983) reported a search for pulsating DB white dwarf stars, classifying twenty nine stars as non-variable. Expanding this search, we acquired time-series photometric observations of another thirteen DB white dwarf stars, which have T_{eff} close to the edges of the DB observed instability strip, plus one DA (H atmosphere white dwarf) during two observing runs at the South African Astronomical Observatory (SAAO), and four DBs at the Observatório Pico

Table 3. Using the distance determined by parallax measurements (second column), we study the best agreement with our fits, deriving the atmosphere composition (third column).

Star	d (pc)	Atmosphere
GD 408	35 ± 6	undetermined
Feige 4	33 ± 10	undetermined
GD 325	35 ± 4	He/H
G 200-39	58 ± 13	pure He
GD 358	37 ± 4	undetermined
L 1573-31	49 ± 7	pure He

dos Dias (OPD) in other three runs, to search for variability. At SAAO, one of us (GH) used the 0.75-m telescope in

Table 4. Atmospheric parameter determinations from UV spectra in comparison to those derived by Beauchamp et al. (1999) using optical spectra. The last column shows the best agreement in atmosphere composition using both independent determinations.

Name	UV He	UV He/H	Optical He	Optical He/H	Atmosphere
G 270-124	20 500 ± 130	19 000 ± 100	22 500	20 500	He/H
PG 0112+104	27 000 ± 110	27 000 ± 130	31 500	28 300	He/H
PG 1115+158	23 000 ± 500	22 000 ± 500	25 300	21 800	He/H
PG 1351+489	22 500 ± 190	22 000 ± 150	26 100	22 600	He/H
PG 1445+152	21 500 ± 120	21 000 ± 120	23 600	22 200	He/H
GD 190	22 500 ± 90	21 000 ± 60	21 500	21 000	He/H
GD 358	24 500 ± 130	24 000 ± 50	24 900	24 700	He
PG 1654+160	25 000 ± 550	26 000 ± 1100	27 800	24 300	He/H

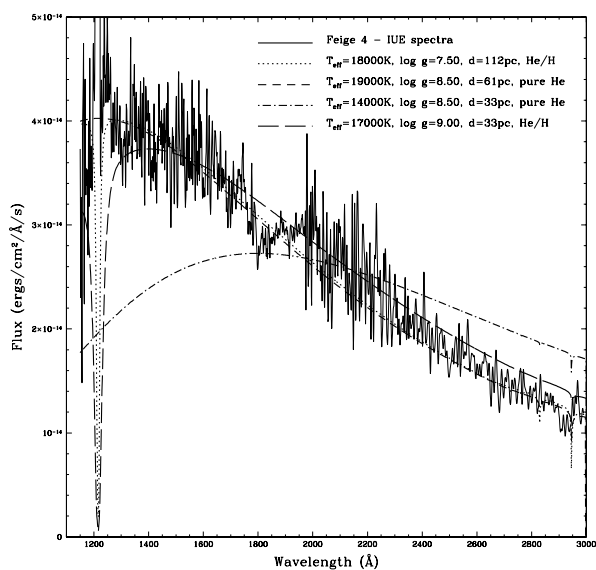


Fig. 1. IUE spectra obtained for Feige 4 (full line) compared with the best models derived leaving all parameters free for a pure He grid (dashed line) at $d = 61$ pc, with $T_{\text{eff}} = 19\,000$ K and $\log g = 8.50$, for a a DB contaminated with H (dotted line), at $d = 112$ pc, with $T_{\text{eff}} = 18\,000$ K and $\log g = 7.50$. Using the parallax distance, ($d = 33$ pc) for pure He grid (dotted-dashed line), the best solution is for $T_{\text{eff}} = 14\,000$ K and $\log g = 8.50$, and for a DB contaminated with H (long dashed line), the atmospheric parameters are $T_{\text{eff}} = 17\,000$ K and $\log g = 9.00$.

April/May 2000 and the 1.0-m telescope in December 2001. At both telescopes, a high-speed CCD photometer (O’Donoghue 1995) was employed. It was operated in full-frame mode on the 0.75-m telescope with 20-s integrations and 3–4 s readout during the measurements in 2000, but in frame-transfer mode with 10-s integrations in 2001. At OPD, we used the 1.6-m telescope in 1986, with a single channel photometer and 5-s integration time. We also observed at OPD in 2004, using the 0.6-m telescope and CCD 101, with 30-s integration, and 7–8 s readout. No filters were used in order to maximize the received light and considering that g-mode pulsations should have the same phase at different wavelengths (e.g. Kepler et al. 2000). We show the observing log in Table 5.

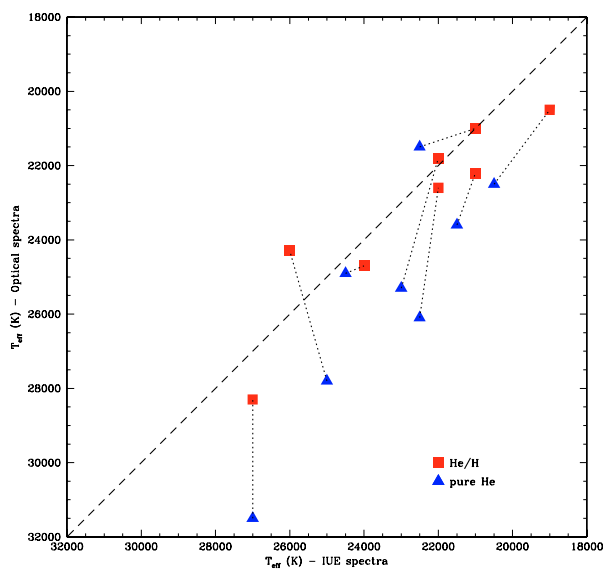


Fig. 2. Comparison between the UV (x -axis) and optical (y -axis) determinations for T_{eff} using pure He models (blue triangles) and DB models contaminated with H (red squares). The dotted lines correspond to the same star. The dashed line delineates 1:1 correspondence between UV and optical spectra.

We reduced the SAAO CCD data with the standard software for this instrument, and carried out photometry by using the program MOMF (Kjeldsen & Frandsen 1992) which uses a combined approach of PSF fitting photometry and aperture corrections on the star-subtracted frames, giving optimal results. Fourier amplitude spectra of the resulting light curves are shown in Fig. 3. For the OPD runs, the detection limits are 3 mma for BPM 17088 and GD 270-124, 2 mma for BPM 17731, and 1.4 mma for L 7-44.

All the seventeen stars are constant within our detection limit. The detection limits are satisfactory for all stars except PG 0949+094, WD 1415+234 (run terminated by cloud) and PG 2234+064, which should be re-observed. WD 1445+152 may also require some additional observations; the highest peak in its amplitude spectrum is somewhat outside the typical range for pulsating white dwarf stars

Table 5. Journal of observations. ΔT is the length of the corresponding observing run.

Star	Run start (UT)	ΔT (h)	# points
BPM 17088	09/09/86, 05:18	1.24	890
BPM 17731	11/09/86, 04:11	3.17	2282
GD 270-124	31/10/86, 22:54	3.37	2423
WD 0853+163	26/04/00, 17:46	1.13	173
WD 1311+129	27/04/00, 21:23	1.51	230
PG 1445+152	28/04/00, 21:18	1.33	195
PG 0949+094	29/04/00, 17:00	1.25	193
PG 1026-056	29/04/00, 18:19	1.15	175
L 151-81A	29/04/00, 23:53	1.61	250
WD 1134+073	30/04/00, 18:15	1.41	213
WD 1332+162	01/05/00, 18:29	1.79	260
WD 1336+123	01/05/00, 20:19	1.43	222
WD 1444-096	01/05/00, 21:48	1.10	168
WD 1415+234	01/05/00, 22:57	0.57	88
PG 2354+159	16/12/01, 18:38	1.07	386
PG 2234+064	17/12/01, 18:57	0.91	326
L 7-44	15/08/04, 00:33	2.61	233

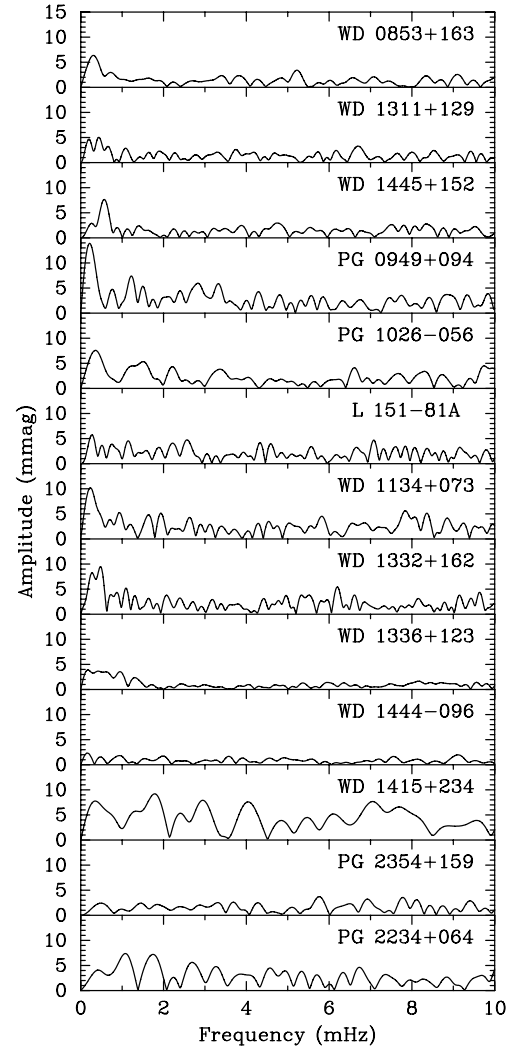
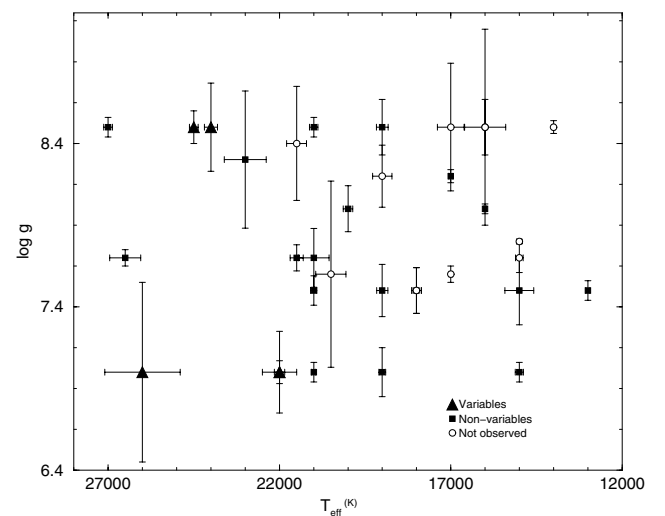
Table 6. Variability classification of the DB stars in our sample. The V is used for variables, NV for non-variables and NO for not observed for variability.

	Stars
V	PG 1115+158, PG 1351+489, PG 1456+103, GD 358, PG 1654+160
NV	Feige 4, G270-124, PG 0112+104, GD 40, BPM 17731, Ton 10, PG 0853+163, GD 303, PG 1311+129, GD 325, PG 1445+152, G 256-18, GD 190, L 7-44, GD 378, G 26-10, LTT 9031 BPM 17088
NO	G 226-32, GD 408, BPM 18164, L 748-70, PG 0948+013, PG 1149-133, PG 1326-037, PG 1411+218, G 200-39, L 1537-31, BPM 26944

but we cannot rule out that it is intrinsic to the star from the present data. We also note that we could not detect variability of the DA white dwarf L 151-81B, but our detection limit (~ 8 mma) is poor. On the other hand, we suspect that the star 2MASS 14581310-6317340, (~ 8 arcsec East of L 151-81AB) is a δ Scuti star, with a 1.3-h period and 23 mmag semi-amplitude.

The variability classification of DB stars is shown in Table 6, where V is used for variables, NV for non-variables, and NO for not observed for variability reported.

Having derived the physical parameters from ultraviolet spectra, and the atmosphere composition for thirteen stars, we are ready to determine the DB instability strip for this homogeneous sample. In Figs. 4 and 5, we show the final determination

**Fig. 3.** Fourier amplitude spectra of the null results of a search for pulsation among DB white dwarf stars.**Fig. 4.** DB instability strip using pure He models for the stars for which we cannot determine atmosphere composition: variables (filled triangle), non-variables (filled squares), and not observed for variability (open circles). There are 2 stars close to the instability strip that have not been observed for variability.

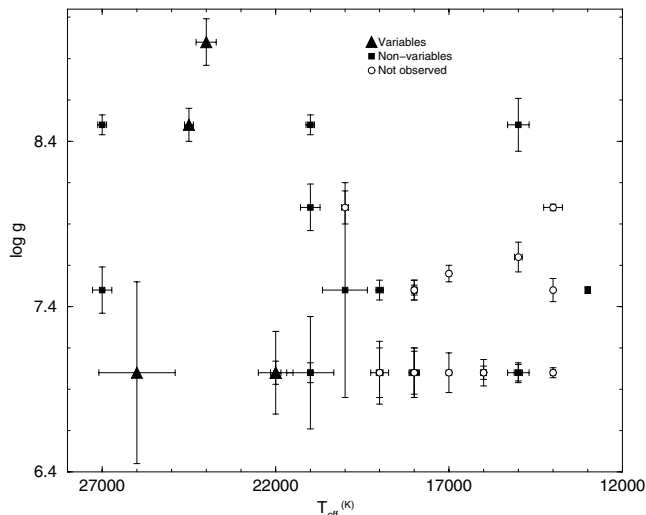


Fig. 5. DB instability strip using H contaminated He models for the stars for which we cannot determine atmosphere composition: variables (filled triangle), non-variables (filled squares), and not observed for variability (open circles). There are 2 stars close to the instability strip that have not been observed for variability.

for T_{eff} and $\log g$ for variables (filled triangle), non-variables (filled squares), and so far not observed by time series photometry (open circles) DB stars. This diagram shows that DBs pulsate in a well-defined temperature range, from $26\,000 \geq T_{\text{eff}} \geq 22\,000$ K. For the stars which we could not determine their atmosphere composition, we used both pure He models and He/H models, respectively. There is a 97% chance that the DB instability strip contains only variable stars. Even if the error bars in T_{eff} were three times larger, there is only a 4% probability of contamination. This probability was calculated by adding the probability of all variables that fall inside the instability strip and all non-variables outside, using Gaussian distributions for our T_{eff} determinations only (no consideration for $\log g$). There are still stars close to the instability strip that have not been searched to our knowledge for variability, and which are crucial for the study of the instability strip.

However, Beauchamp et al.'s (1999) optical spectra fitting found non-variables inside the instability strip. In this sense, for a true determination of the DB instability strip it is necessary to fit the optical and UV spectra simultaneously, to analyze the possible differences to convection prescription.

5. Concluding remarks

We used model atmospheres with $ML2/\alpha = 0.6$ to derive atmospheric parameters (T_{eff} and $\log g$) and distances for thirty four DB stars with available IUE re-calibrated spectra. Our model grid fit well the spectra. Another important conclusion is that atmospheric contamination with H is not directly proportional to T_{eff} for DB stars, based on our determination for eleven stars, which has been a suggestion to explain the DB gap by convection dragging H upwards. We also find no DB stars inside the DB gap.

Acknowledgements. Financial support: CAPES/UT grant, CNPq fellowship.

References

- Althaus, L. G., & Benvenuto, O. G. 1997, *ApJ*, 477, 313
- Althaus, L. G., Serenelli, A. M., Panci, J. A., et al. 2005, *A&A*, 435, 631
- Beauchamp, A., et al. 1999, *ApJ*, 516, 887
- Bergeron, P., Saumon, D., & Wesemael, F. 1995, *ApJ*, 443, 764
- Bergeron, P., Leggett, S. K., & Ruiz, M. T. 2001, *ApJS*, 133, 413
- Corsico, A. H., & Althaus, L. G. 2004, *A&A*, 428, 159
- Finley, D. S., Koester, D., & Basri, G. 1997, *ApJ*, 488, 375
- Hansen, B., & Liebert, J. 2003, *ARA&A*, 41, 465
- Holberg, J. B., Barstow, M. A., & Burleigh, M. R. 2003, *ApJS*, 147, 145
- Kepler, S. O., Robinson, E. L., Koester, D., et al. 2000, *ApJ*, 539, 379
- Kjeldsen, H., & Frandsen, S. 1992, *PASP*, 104, 413
- Koester, D., & Vauclair, G. 1997, *White dwarfs*, ASSL 214, 429
- Metcalf, T. S. 2003, *ApJ*, 587, L43
- Metcalf, T. S. 2005, *MNRAS*, 363, L86
- Montgomery, M. H., & Winget, D. E. 2000, *Baltic Astron.*, 9, 23
- Nitta, A., et al. 2005, in prep.
- O'Donoghue, D. 1995, *Baltic Astronomy*, 4, 519
- Provencal, J. L., Shipman, H. L., Thejll, P., & Vennes, S. 2000, *ApJ*, 542, 1041
- Robinson, E. L., & Winget, D. E. 1983, *PASP*, 95, 386
- van Altena, W. F., Lee, J. T., & Hoffleit, E. D. 2001, *VizieR Online Data Catalog*, 1238, 0
- Winget, D. E., Robinson, E. L., Nather, R. D., Fontaine, G. 1982, *ApJ*, 262, L11
- Winget, D. E., Sullivan, D. J., Metcalfe, T. S., Kawaler, S. D., & Montgomery, M. H. 2004, *ApJ*, 602, L109
- Wolff, B., Koester, D., Montgomery, M. H., & Winget, D. E. 2002, *A&A*, 388, 320